Photocurrent in nanostructures with asymmetric antidots: Exactly solvable model

M. V. Entin and L. I. Magarill
Institute of Semiconductor Physics, Siberian Branch of Russian Academy of Sciences, Novosibirsk, 630090, Russia
(Received 20 December 2005; revised manuscript received 16 March 2006; published 19 May 2006)

The steady current induced by electromagnetic field in a 2D system with asymmetric scatterers is studied. The scatterers are assumed to be oriented cuts with one diffusive and another specular sides. Besides, the existence of isotropic impurity scatterers is assumed. This simple model simulates the lattice of half-disk which have been studied numerically recently. The model allows the exact solution in the framework of the kinetic equation. The direct current is expressed via the second-order response in electric field. The photogalvanic tensor contains both responses to linear and circular polarization of electromagnetic field. The model possesses nonanalyticity with regards to the rate of impurity scattering.

DOI: 10.1103/PhysRevB.73.205206 PACS number(s): 73.40.−c, 73.50.Bk, 73.50.Pz

I. INTRODUCTION

Nowadays technology allows to fabricate artificial arrays of antidot scatterers which form superlattices in semiconductor heterostructures with a two dimensional electron gas (2DES) (see, e.g., Refs. 1–4 and references therein). The size of antidots can be varied from a few microns to a few tens of nanometers at a typical electron density $n_e \sim 10^{12}$ cm^{-2}. Superlattices with circular antidots (disks), known as the Galton board,[5] have been realized in experiments.[1–4] The mathematical theorems of Sinai guarantee that the classical dynamics of electrons in such structures is chaotic.[6] The effects of chaotic dynamics and contributions of unstable periodic orbits on electron conductivity have been clearly seen experimentally. They were also analyzed by theoretical methods and numerical simulations in great detail.[7] The irradiation of such superlattices by a microwave field[8] opens interesting possibilities for microwave control of electron current in nanostructures. These systems of relatively large period are classical, and the periodic potential is the source of electron scattering.

Unlike arrays of symmetric antidots, studied experimentally in early works, more sophisticated systems were for a long time out of attention. Meanwhile, systems without inversion symmetry are capable to rectify the electric current. The stationary current in homogeneous media affected by light in the absence of any dc voltage called the *photogalvanic effect* (PGE) was studied since the end of the seventies.[9–14] Similar direct current caused by temporal irreversibility due to simultaneous action of two electromagnetic fields with frequencies ω and 2ω is known as the coherent photogalvanic effect (CPGE).[15]

Appearance of directed transport without obvious directed forces is also known as ratchet effect which has a long history. For example, the behavior of a ratchet under the influence of thermal fluctuations was considered in the textbook by Feynman, Leighton, and Sands[16] in connection with the problem of reversibility in statistical mechanics. Recently the ratchet problem attracted a great interest of the scientific community.[17,18] In fact the photogalvanic effect corresponds to a ratchet subjected to weak alternating force with zero mean. Such ratchets have been observed in various physical systems including Josephson junction arrays,[19–21] cold atoms,[22] macroporous silicon membranes,[23] microfluidic channels,[24] and other systems. The growing interest to ratchets is strongly stimulated by their possible applications to biological systems.[17,25] In this sense the artificial asymmetric nanostructures, as those discussed in Refs. 26–28 and here, can serve as a prototype for understanding of photocurrent properties in biomolecules. The results obtained for ratchets induced by microwave fields in nanostructures can be also used for understanding of directed transport created by ac fields in molecular electronics.[29]

Relatively recently an artificial lattice of asymmetric antidots (triangles) participating in transport as scatterers of electrons was realized experimentally. It exhibited the direct current induced by alternating electric field.[30] The effect of such type was considered theoretically in Ref. 31 by means of the classical kinetic equation for the system with weak asymmetric periodic lateral potential.

Another case of superlattices of asymmetric antidots (semidisks oriented in one direction or the semidisk Galton board) has been proposed and analyzed theoretically[26–28] by simulations of motion of a particle subjected to alternating force with zero means and collisions with hard-wall antidots. It has been shown that a microwave radiation creates the directed flow of electrons. The velocity of this flow v_f is proportional to a friction coefficient while the direction of current depends on the microwave polarization. The directed transport induced by a microwave field appears also for an ensemble of noninteracting particles in a thermal equilibrium at temperature T. This effect is absent in structures with circular antidots due to symmetry conservation. Recently, semidisk Galton board realized experimentally[32] exhibited the rectification of high-frequency electric field.

In Refs. 26–28 the properties of photocurrent in asymmetric nanostructures have been explained on the basis of heuristic arguments and extensive numerical simulations. However, the analytical theory of the effect still needs to be developed. This aim is reached in this paper with the help of a kinetic equation approach applied to a specific model of asymmetric scatterers (cuts model). This approach allows us to obtain analytical dependence of photocurrent properties on system parameters.

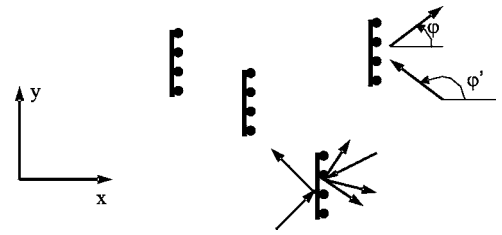

FIG. 1. Considered model system. Cuts have specular left sides and diffusive right sides. This produces anisotropy of scattering resulting in the photocurrent.

II. KINETIC EQUATION APPROACH

Here we study a simple model of anisotropic 2D artificial scatterers, which permits the analytical consideration in the framework of kinetic equation approximation and leads to the PGE. The kinetic equation was used in a number of papers devoted to photogalvanic effect. Unlike the particle dynamics method, this way suggests the developed chaos picture where ergodicity of motion is achieved. At the same time it is free from the voluntary assumptions about the particle friction used in Refs. 26 and 27.

The system under consideration contains randomly distributed oriented scatterers. The scatterers are assumed to be segments of the length D oriented along the y axis; one side (left) of the segment is specular and the other side is diffusive (see Fig. 1). The concentration of scatterers N is supposedly low: $ND^2 \ll 1$. In this approximation the kind of spatial distribution of scatterers (random or periodic) is of no importance. Besides, to limit the possible divergency of the result we include isotropic impurity scattering into our model.

This system can be considered as a simplification of the semicircle model studied in Refs. 26 and 27. In fact, the diffusive side of the cut scatters particles like round side of the semicircle, if not to pay attention to the difference between randomized (in our case) and deterministic (in semicircle case) motion. The advantage of "cuts" model is its exact solvability.

The kinetic equation reads as

$$\frac{\partial f}{\partial t} + \hat{F}f = \hat{I}f, \tag{1}$$

where $f(p,\varphi)$ is the distribution function, $\mathbf{p}=p(\cos\varphi,\sin\varphi)$ is the electron momentum. The term $(\hat{F}f)$ represents the action of electric field $\mathbf{E}(t)=\mathrm{Re}(\mathbf{E}_\omega e^{-i\omega t})$ of the electromagnetic wave with the complex amplitude $\mathbf{E}_\omega=\mathbf{E}^*_{-\omega}$

$$\hat{F} \equiv \frac{1}{2}\hat{F}_\omega e^{i\omega t} + \text{c.c.} = -e\left[E_x\left(\cos\varphi\frac{\partial}{\partial p} - \frac{\sin\varphi}{p}\frac{\partial}{\partial\varphi}\right) + E_y\left(\sin\varphi\frac{\partial}{\partial p} + \frac{\cos\varphi}{p}\frac{\partial}{\partial\varphi}\right)\right]. \tag{2}$$

As it will be seen further, the acceleration in the y direction cannot be limited by the scattering on segments only because electrons moving in this direction do not relax. This is why we have not restricted our consideration by the collisions with cuts only but have also taken into account the impurity scattering. Hence the collision integral $\hat{I}f \equiv \hat{I}_i f + \hat{I}_c f$ is assumed to consist of impurity-induced $\hat{I}_i$ and segment-induced $\hat{I}_c$ collision integrals. The segment-induced collision integral

$$\hat{I}_c f = \int_0^{2\pi} d\varphi' [W(\varphi',\varphi)f(p,\varphi') - W(\varphi,\varphi')f(p,\varphi)] \tag{3}$$

is determined by the scattering probability on the cuts $W(\varphi',\varphi)$.

The collision integral should conserve the number of electrons and vanish for any isotropic distribution function. These conditions imply [we keep in mind that the number of electrons colliding with the cut is proportional to $(pD/m)\cos\phi'$]

$$W(\varphi',\varphi) = \frac{1}{\tau}\Big[\cos\varphi'\,\theta(\cos\varphi')\,\delta(\varphi'+\varphi-\pi) - \tfrac{1}{2}\cos\varphi'\cos\varphi\,\theta(\cos\varphi)\,\theta(-\cos\varphi')\Big], \tag{4}$$

where $\tau=(DNv)^{-1}$ is the corresponding characteristic time, $\theta(x)$ is the Heaviside function; the first and the second terms in the square brackets correspond to the specular reflection on the left side and diffusive scattering on the right side of a cut, respectively.

The impurity scattering is suggested to be isotropic

$$\hat{I}_i f = -\frac{1}{\tau_i}(f - \langle f\rangle), \tag{5}$$

where $\langle\cdots\rangle$ means average over angles, τ_i is the relaxation time corresponding to additional isotropic scattering.

We shall solve the kinetic equation (1) in the second order on electric field. In the elastic approximation the collision operator is degenerate because its action on the isotropic function gives zero; thus this operator has eigenfunctions with zero eigenvalue and the solution of Eq. (1) is ambiguous. However, if to project the Hilbert space of distribution functions on the subspace with zero angular average, the corresponding projection of the scattering operator becomes nondegenerate. So if to consider only the distribution functions with zero mean, the elastic scattering operator remains nondegenerate and can be treated as full relaxation operator. Inelastic scattering controls only isotropic part of the distribution function which (if it is weaker than elastic one) has no impact on the PGE.

In the second order on alternating electric field the steady current density is described by the phenomenological expression

$$j_i = \alpha_{ijk}E_{\omega,j}E_{-\omega,k}. \tag{6}$$

The symmetry of the considered system allows the following nonzero components of the photogalvanic tensor α_{ijk}:

$$\alpha_{xxx}, \alpha_{xyy}, \alpha_{yxy} = \alpha^*_{yyx}. \tag{7}$$

From Eq. (6) it follows that components α_{xxx} and α_{xyy} are real. The same is valid for all components of α_{ijk} in the static limit $(\omega=0)$.

Equation (6) is specified as

$$j_x = \alpha_{xxx}|E_x|^2 + \alpha_{xyy}|E_y|^2,$$

$$j_y = \mathrm{Re}(\alpha_{yxy})(E_x E_y^* + E_x^* E_y) + \mathrm{Im}(\alpha_{yxy})[\mathbf{E}\mathbf{E}^*]_z. \quad (8)$$

The components α_{xxx}, α_{xyy}, and $\mathrm{Re}(\alpha_{yxy})$ determine the response to the linear-polarized light. For linear polarization along x or y axes the current flows along x direction; the current in y direction appears for tilted linear-polarized electric field. In the case of circular polarization the y component of the current is determined by $\mathrm{Im}(\alpha_{yxy})$ (the circular photogalvanic effect) and by the sign of the rotation, while x component of the current is the sum of responses to x and y linear polarized light and does not depend on the sign of $[\mathbf{E}\mathbf{E}^*]_z$. Notice that the circular photogalvanic effect vanishes if the frequency $\omega \to 0$.

The formal solution of Eq. (1) in the second order in electric field is

$$f_2 = \left(\frac{\partial}{\partial t} - \hat{I}\right)^{-1} \hat{F} \left(\frac{\partial}{\partial t} - \hat{I}\right)^{-1} \hat{F} f_0, \quad (9)$$

where $f_0 = 1/[\exp(\epsilon-\mu)/T+1]^{-1}$ is the equilibrium distribution function ($\epsilon = p^2/2m$), μ is the chemical potential, T is the temperature. The kernel of the inverse operator in frequency representation $G^\omega(\varphi', \varphi)$ satisfies the equation $(-i\omega + \hat{I})G^\omega(\varphi, \varphi') = \delta(\varphi - \varphi')$ which can be solved exactly

$$\begin{aligned} G^\omega(\varphi, \varphi') = -\tau \Bigg\{ & \frac{\delta(\varphi - \varphi')}{|\cos\varphi| + \xi} \\ & + \frac{|\cos\varphi|}{2} \frac{\cos^2\varphi' - \xi\cos\varphi'\,\theta(-\cos\varphi')}{(|\cos\varphi| + \xi)(|\cos\varphi'| + \xi)^2[1 - \Phi(\xi)]} \\ & + \frac{\theta(-\cos\varphi)}{(|\cos\varphi| + \xi)^2} \Bigg[-\cos\varphi\,\delta(\varphi + \varphi' - \pi) \\ & + \xi\cos\varphi \frac{\cos^2\varphi' - \xi\theta(-\cos\varphi')\cos\varphi'}{2(|\cos\varphi'| + \xi)^2[1 - \Phi(\xi)]} \Bigg] \Bigg\}. \end{aligned} \quad (10)$$

Here $\xi = -i\omega\tau + \tau/\tau_i$

$$\Phi(x) = -\pi x + 2 - \frac{1}{1-x^2} - x^2 \frac{3 - 2x^2}{1 - x^2} \Phi(1, x). \quad (11)$$

The functions $\Phi(n, \xi)$ denote the integrals expressing through elementary functions

$$\Phi(n, x) = \int_0^{\pi/2} \frac{dt}{(\cos t + x)^n},$$

$$\Phi(1, x) = -\frac{2}{\sqrt{1 - x^2}} \mathrm{arctanh}\left(\frac{-1 + x}{\sqrt{1 - x^2}}\right). \quad (12)$$

The stationary part of the correction f_2 can be written as

$$\bar{f}_2 = \tfrac{1}{4}\hat{G}^0(\hat{F}_\omega \hat{G}^{-\omega} \hat{F}_{-\omega} + \hat{F}_{-\omega} \hat{G}^\omega \hat{F}_\omega) f_0, \quad \hat{G}^0 \equiv \hat{G}^{\omega=0}. \quad (13)$$

The static current reads

$$j_i = -2e \int \frac{d^2p}{(2\pi)^2} v_i \bar{f}_2. \quad (14)$$

The photogalvanic tensor is expressed via partial tensor $\tilde{\alpha}_{ijk}$ for electrons with given p

$$\alpha_{ijk} = \frac{e^3}{2m\pi^2} \int_0^\infty dp\,\tau^2 \left(-\epsilon \frac{\partial f_0}{\partial \epsilon}\right) \tilde{\alpha}_{ijk}. \quad (15)$$

In the degenerate case the partial tensor itself determines the total tensor α_{ijk}

$$\alpha_{ijk}(T = 0, \epsilon_F) = \alpha_0\, \tilde{\alpha}_{ijk}|_{p=p_F}, \quad (16)$$

where $\alpha_0 = e^3/(4\pi^2 N^2 D^2 v_F)$, $v_F = p_F/m$, p_F is the Fermi momentum, $\epsilon_F = p_F^2/2m$ is the Fermi energy. At finite temperatures T

$$\alpha_{ijk}(T, \mu) = \int d\epsilon \left(-\frac{\partial f_0}{\partial \epsilon}\right) \alpha_{ijk}(T = 0, \epsilon_F = \epsilon). \quad (17)$$

The dimensionless tensor $\tilde{\alpha}_{ijk}$ can be presented as a function of parameters $\zeta = \tau/\tau_i$ and $\xi = \zeta - i\Omega$ ($\Omega = \omega\tau$).

III. ANALYTICAL RESULTS

Substituting the stationary part of the distribution function (13) into the expression (14) and using the Green function (10) we find after integration

$$\begin{aligned} \tilde{\alpha}_{xxx}(\xi, \zeta) = {} & [B(\zeta) - B(\xi)] \left(1 - \frac{\pi\zeta}{2} + \frac{\zeta^4 + \zeta\xi - 2\zeta^3\xi}{(\xi - \zeta)^2} \Phi(1, \zeta) - \frac{\zeta\xi - 2\zeta\xi^3 + \xi^4}{(\xi - \zeta)^2} \Phi(1, \xi) + \xi^2 \frac{\xi^2 - 1}{\xi - \zeta} \Phi(2, \xi)\right) \\ & + B(\zeta)B(\xi) \left(-\frac{\pi\zeta}{2} - \frac{2\zeta(\zeta^4 - \zeta\xi - 3\zeta^3\xi - \xi^2 + 4\zeta^2\xi^2)}{(\xi - \zeta)^3} \Phi(1, \zeta) + \frac{2\xi[\xi^4 + \zeta^2(-1 + 4\xi^2) - \zeta(\xi + 3\xi^3)]}{(\xi - \zeta)^3} \Phi(1, \xi)\right. \\ & \left. - \frac{\zeta^2(\zeta^3 + \xi - 2\zeta^2\xi)}{(\xi - \zeta)^2} \Phi(2, \zeta) + \frac{\xi^2[\xi - 4\xi^3 + \zeta(-4 + 7\xi^2)]}{(\xi - \zeta)^2} \Phi(2, \xi) + \frac{2\xi^3(-1 + \xi^2)}{\xi - \zeta} \Phi(3, \xi)\right) + \text{c.c.}, \end{aligned} \quad (18)$$

$$\tilde{\alpha}_{xyy} = 1 - 3B(\zeta) + \frac{\pi\zeta[4B(\zeta)-1]}{2} + [3\zeta^3\xi - \zeta^4 - \zeta\xi + \xi^2 - 2\zeta^2\xi^2 + B(\zeta)(5\zeta^4 + 3\zeta\xi - 15\zeta^3\xi - 3\xi^2 + 10\zeta^2\xi^2)]\frac{\zeta\Phi(1,\zeta)}{(\xi-\zeta)^3}$$
$$+ \frac{\xi[\zeta^2 - \zeta\xi - 2\zeta^2\xi^2 + 3\zeta\xi^3 - \xi^4 + B(\zeta)(3\zeta\xi - 3\zeta^2 + 10\zeta^2\xi^2 - 15\zeta\xi^3 + 5\xi^4)]\Phi(1,\xi)}{(\xi-\zeta)^3} + \frac{\zeta^2 B(\zeta)(\zeta^3 + \xi - 2\zeta^2\xi)\Phi(2,\zeta)}{(\xi-\zeta)^2}$$
$$+ \frac{\xi^2[\zeta - \xi - \zeta\xi^2 + \xi^3 + B(\zeta)(4\xi - 5\zeta + 8\zeta\xi^2 - 7\xi^3)]\Phi(2,\xi)}{(\xi-\zeta)^2} + \frac{2\xi^3 B(\zeta)(\xi^2-1)\Phi(3,\xi)}{\xi-\zeta}, \tag{19}$$

$$\tilde{\alpha}_{yxy}(\xi,\zeta) = [(\zeta-\xi)(-2\zeta\xi + \pi^2\zeta(\zeta-\xi)(-1+\xi^2) + \pi\{-\xi + \zeta[2 + (\zeta - 3\xi)\xi]\} + \xi\Phi(1,\xi)[-(\pi\xi) + 2\zeta^2(1+\pi\xi)(-1+2\xi^2)$$
$$+ \zeta^3(\pi - 2\pi\xi^2) + 2\zeta\xi(2 + 2\pi\xi - 3\xi^2 - 2\pi\xi^3) + 4\zeta\xi^3(-1+\xi^2)\Phi(1,\xi)]$$
$$+ \zeta(\zeta - 2\xi)\Phi(1,\zeta)[-2(-1+\zeta^2)\xi - \pi(-1+2\zeta^2)(-1+\xi)(1+\xi) + 2\xi(-\xi^2 + \zeta^2(-1+2\xi^2))\Phi(1,\xi)]]$$
$$\times\{2(\zeta-\xi)^2[\pi + \xi - \pi\xi^2 + \xi(-3+2\xi^2)\Phi(1,\xi)]\}^{-1}$$
$$- \left(\frac{1}{2(\zeta-\xi)^3}\{(\zeta-\xi)[-8 + \pi\zeta^3 - 2\zeta^2(1+\pi\xi) + \zeta\xi(10+\pi\xi)] - 2[\zeta^5 + 2\xi - 3\zeta^2\xi - 3\zeta^4\xi + \zeta(2-4\xi^2)\right.$$
$$\left. + \zeta^3(-1+6\xi^2)]\Phi(1,\zeta) + 2[-(\xi(-2+\xi^2)) + \zeta^2\xi(-2+3\xi^2) + \zeta[2 - 5\xi^2 + \xi^4)]\Phi(1,\xi)\}\right)^*. \tag{20}$$

The function $B(\xi)$ is given by

$$B(\xi) = \frac{1}{2}\frac{(-1+\xi^2)[-\pi + 2\xi\Phi(1,\xi)]}{\pi + \xi - \pi\xi^2 + \Phi(1,\xi)\xi(2\xi^2-3)}. \tag{21}$$

The quantity $\tilde{\alpha}_{xxx}$ has a static ($\omega\to 0$) limit

$$\tilde{\alpha}_{xxx}(\zeta,\zeta) = -\zeta B(\zeta)^2[\pi - 8\zeta\Phi(1,\zeta) + 2(-1+6\zeta^2)\Phi(2,\zeta) + 4\zeta(1-2\zeta^2)\Phi(3,\zeta) + 2\zeta^2(\zeta^2-1)\Phi(4,\zeta)]. \tag{22}$$

If additionally $\zeta\to 0$

$$\tilde{\alpha}_{xxx}(\zeta,\zeta) \approx \frac{1}{6} - \frac{1}{3\pi}\zeta\ln(\zeta/2) - \zeta\frac{(4+3\pi^2)}{12\pi} + \cdots. \tag{23}$$

The case of a clean sample gives the limit 1/6. The positive slope of the function $\tilde{\alpha}_{xxx}(\zeta,\zeta)$ change to negative at very low numerical value of $\zeta \sim 2\exp(-1-3\pi^2/4)$. This behavior is plotted on the inset in Fig. 2.

If $\zeta\to\infty$

$$\tilde{\alpha}_{xxx}(\zeta - i\Omega, \zeta) \approx \frac{\pi}{8\zeta^3} + \cdots. \tag{24}$$

If the frequency goes to infinity

$$\tilde{\alpha}_{xxx}(\zeta, \zeta + i\Omega) = \frac{1}{\Omega^2}F(\zeta),$$

$$F(\zeta) = \frac{\pi\zeta}{4}, \quad \text{if } \zeta\to 0,$$

$$F(\zeta) = \frac{\pi}{24\zeta}, \quad \text{if } \zeta\to\infty. \tag{25}$$

The function $F(\zeta)$ has the maximum equal to 0.0717 at $\zeta = 0.455$. For finite ω and $\zeta\to 0$ $\tilde{\alpha}_{xxx}\to 0$.

The static limit of $\tilde{\alpha}_{xyy}$ is given by

$$\tilde{\alpha}_{xyy}(\zeta,\zeta) = -[2\pi^2\zeta(\zeta^2-1)^2 + \pi(1 + 2\zeta^4 - 6\zeta^2) + 2(\zeta + 2\zeta^5 - 2\zeta^3) + \Phi(1,\zeta)(8\zeta^6 - 16\zeta^4 - 6\zeta^3 + 11\zeta^2) + 4\zeta^3(2\zeta^4 - 4\zeta^2 + 3)\Phi^2(1,\zeta)]\{2(\zeta^2-1)[\pi + \zeta - \pi\zeta^2 + \zeta\Phi(1,\zeta)(2\zeta^2-3)]\}^{-1}, \tag{26}$$

which yields

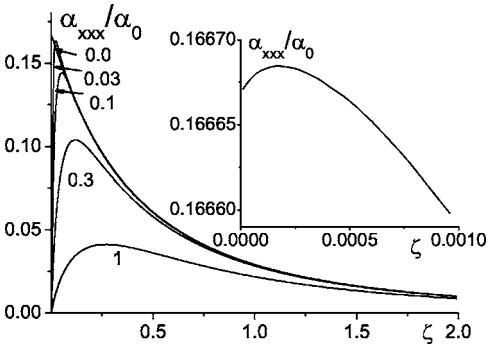

FIG. 2. The dependence of $\tilde{\alpha}_{xxx}$ on the parameter $\zeta = \tau/\tau_i$ for different frequencies $\Omega = \omega\tau = 1, 0.3, 0.1, 0.03, 0$ (marked on curves); $\alpha_0 = e^3/(4\pi^2 v_F N^2 D^2)$. Inset: The dependence of $\tilde{\alpha}_{xxx}$ for small values of the parameter ζ at $\Omega = 0$. The sign of the curve slope changes at very low ζ in accord with the asymptotic Eq. (23).

$$\tilde{\alpha}_{xyy}(\zeta,\zeta) \approx -\frac{1}{2} + \frac{\zeta}{2\pi}\left(3\ln\frac{\zeta}{2} + 3 + 2\pi^2\right) + \cdots \quad \text{if } \zeta \to 0. \tag{27}$$

The function $\tilde{\alpha}_{xyy}(\zeta,\zeta)$ [similarly to $\tilde{\alpha}_{xxx}(\zeta,\zeta)$] has a singularity at $\zeta=0$ and changes the sign of slope at very low ζ.

For large ζ we have

$$\tilde{\alpha}_{xyy}(\zeta+i\Omega,\zeta) \approx -\frac{5\pi}{24\zeta^3} + \cdots \quad \text{if } \zeta \to \infty. \tag{28}$$

If $\zeta \to 0$

$$\tilde{\alpha}_{xyy}(\zeta+i\Omega,\zeta) \approx -\pi\zeta\left(\frac{1+2\Omega^2}{2\Omega\sqrt{1+\Omega^2}} - 1\right). \tag{29}$$

The high-frequency behavior of $\tilde{\alpha}_{xyy}(\zeta+i\Omega,\zeta)$ is

$$\tilde{\alpha}_{xyy} \approx \frac{\zeta^2(1-\zeta^2)}{2\Omega^2}\frac{3\pi - 4\zeta - 2\pi^2\zeta - 2\pi\zeta^2 + 2\pi^2\zeta^3 + (8\pi\zeta^2 - \pi + 4\zeta^3 - 8\pi\zeta^4)\Phi(1,\zeta) + 8\zeta^3(\zeta^2-1)\Phi(1,\zeta)^2}{\pi(\zeta^2-1) - \zeta + \zeta(3-2\zeta^2)\Phi(1,\zeta)}, \tag{30}$$

with asymptotics

$$\tilde{\alpha}_{xyy} \approx -\frac{\zeta^2}{2\Omega^2}\left(3 + \ln\frac{\zeta}{2}\right)\cdots \quad \text{for } \zeta \ll 1, \tag{31}$$

and

$$\tilde{\alpha}_{xyy} \approx \frac{\pi}{24\zeta\Omega^2} + \cdots \quad \text{for } \Omega \gg \zeta \gg 1. \tag{32}$$

In the static limit the component $\tilde{\alpha}_{yxy}$ takes the form

$$\begin{aligned}\alpha_{yxy}(\zeta,\zeta) = {} & \frac{1}{6\zeta^2(\zeta^2-1)^3}(2(\zeta^2-1)[2\zeta^4 - 1 - \zeta^2 + 3\zeta^2\Phi(1,\zeta)] \\ & - 3\zeta^2\{(\zeta^2-1)[16\zeta^2 - 11 - 8\zeta^4 + 4\pi\zeta(\zeta^2-1)^2] \\ & + (15\zeta^2 - 6 - 20\zeta^4 + 8\zeta^6)\Phi(1,\zeta)\}B(\zeta)).\end{aligned} \tag{33}$$

For small or large values of ζ we have

$$\tilde{\alpha}_{yxy}(\zeta,\zeta) \approx -\frac{1}{3\zeta^2} + \cdots \quad \text{if } \zeta \ll 1,$$

$$\tilde{\alpha}_{yxy}(\zeta,\zeta) \approx -\frac{\pi}{3\zeta^3} + \cdots \quad \text{if } \zeta \gg 1. \tag{34}$$

For large Ω

$$\mathrm{Re}(\tilde{\alpha}_{yxy}) \approx \frac{F_1(\zeta)}{\Omega^2}, \quad \mathrm{Im}(\tilde{\alpha}_{yxy}) \approx \frac{F_2(\zeta)}{\Omega^3}, \tag{35}$$

$$\begin{aligned}F_1(\zeta) = {} & -\frac{1}{4}\{20 - 48\zeta^2 + \pi^2(1-4\zeta^2) + 6\pi\zeta(-1+4\zeta^2) \\ & + 2[26\zeta^2 - 4 - 24\zeta^4 + \pi\zeta(4\zeta^2-3)]\Phi(1,\zeta)\},\end{aligned} \tag{36}$$

$$\begin{aligned}F_2(\zeta) = {} & \frac{1}{24}[\pi^2(3\zeta - 12\zeta^3) - 96\zeta(\zeta^2-4) + 2\pi(25 - 88\zeta^2 \\ & + 24\zeta^4) - 2\zeta(144 + 9\pi\zeta - 224\zeta^2 - 12\pi\zeta^3 \\ & + 48\zeta^4)\Phi(1,\zeta)].\end{aligned} \tag{37}$$

For small and large ζ this gives

$$\mathrm{Re}(\tilde{\alpha}_{yxy}) \approx \frac{1}{\Omega^2}\left[-5 - \frac{\pi^2}{4} - 2\ln\left(\frac{\zeta}{2}\right)\right], \quad \text{if } \zeta \to 0,$$

$$\mathrm{Re}(\tilde{\alpha}_{yxy}) \approx -\frac{\pi}{6\Omega^2\zeta}, \quad \text{if } \zeta \to \infty. \tag{38}$$

$$\mathrm{Im}(\tilde{\alpha}_{yxy}) \approx \frac{1}{\Omega^3}\left[\frac{25\pi}{12} + \zeta\left(16 + \frac{\pi^2}{8} + 12\ln\frac{\zeta}{2}\right)\right], \quad \text{if } \zeta \to 0,$$

$$\mathrm{Im}(\tilde{\alpha}_{yxy}) \approx \frac{1}{\Omega^3}\left(\frac{\pi}{12} + \frac{76}{45\zeta}\right), \quad \text{if } \zeta \to \infty. \tag{39}$$

IV. NUMERICAL RESULTS AND DISCUSSION

Figures 2–6 represent all components of $\tilde{\alpha}_{ijk}$ calculated according Eqs. (18)–(20) at $T=0$ *versus* parameter $\zeta=\tau/\tau_i$ for different frequencies. These curves show the dependencies of α_{ijk} on the rate of impurity scattering. The sign of coefficient $\tilde{\alpha}_{xxx}$ is positive, while the other coefficients change sign. In accord with the found asymptotics all com-

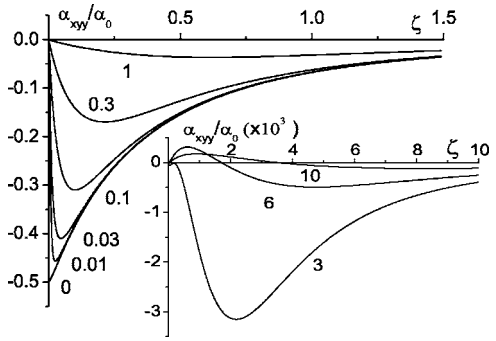

FIG. 3. The behavior of α_{xyy} as function of ζ. For large ζ the component $\alpha_{xyy} \to 0$. For all finite frequencies Ω the coefficient α_{xyy} tends to zero for $\zeta \to 0$. If $\Omega=0$ and $\zeta \to 0 \alpha_{xyy} \to 0.5$. Inset: The dependence of α_{xyy} on ζ for large Ω. The behavior of α_{xyy} at small ζ accords with the Eqs. (30)–(32).

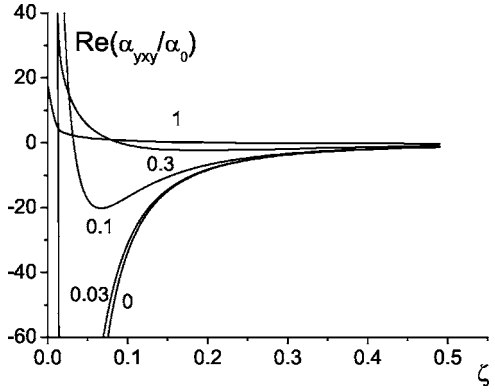

FIG. 4. The dependence of linear photogalvanic coefficient $\mathrm{Re}(\tilde{\alpha}_{yxy})$ on ζ for the same parameters Ω as in Fig. 2. For finite frequency $\tilde{\alpha}_{yxy}$ has a finite limit at $\zeta \to 0$.

ponents tend to zero for $\zeta \to \infty$ and exhibit nonanalytical behavior at $\zeta = 0$.

Asymptotic behavior $\tilde{\alpha} \propto \zeta^{-3}$ (or $\alpha \propto \tau^{-1}$) at large ζ follows from the odd dependence of the current on the asymmetric scattering on the cuts that results in the proportionality of the current to the scattering rate on cuts for low their concentration. This asymptotics corresponds to the case of weak asymmetric scattering usually considered in the theory of PGE.

The value $\tilde{\alpha}_{ijk}(0,0)$ depends on the order of limit $\omega \to 0$, $1/\tau_i \to 0$: for example, $\tilde{\alpha}_{xxx} \to 1/6$ if first $\omega \to 0$ next $1/\tau_i \to 0$, otherwise $\tilde{\alpha}_{xxx} \to 0$. Such behavior results from the absence of relaxation of electrons moving along y axis. The state with $p_x = 0$ plays role of a drain for electrons. These electrons do not participate in the transport along x axis, but due to absence of relaxation they accumulate in the state $p_x = 0$; this suppresses the distribution function with finite p_x, and $j_x \to 0$. On the contrary, the transport along y axis diverges due to the same reason.

For linear polarized electric field the signs of current components depend on the direction of polarization. Physically, this can be explained by the effective increase of the mean-squared component of electron momentum along field and subsequent increase (decrease) of scattering on the cuts. Let electron with a momentum $\mathbf{p} = (\pm p, 0)$ impacts with a cut. The change of momentum are equal to $-2p$ for an electron with the momentum $\mathbf{p} = (p, 0)$ and $(1 + 2/\pi)p$ for an electron

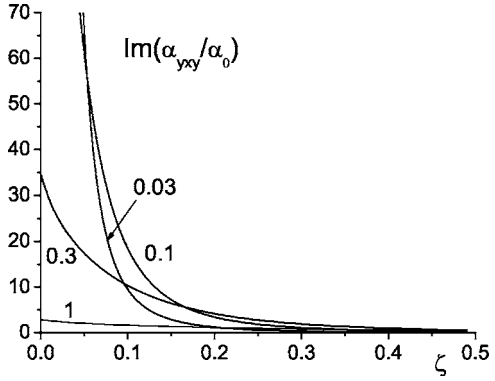

FIG. 5. The dependence of circular photogalvanic coefficient $\mathrm{Im}(\tilde{\alpha}_{yxy})$ for the same parameters Ω as in Fig. 2.

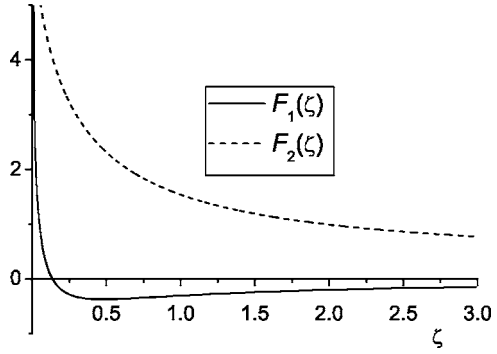

FIG. 6. Asymptotics of photogalvanic coefficient $\tilde{\alpha}_{yxy} = F_1(\zeta)/\Omega^2 + iF_2(\zeta)/\Omega^3$ for large Ω, according to the Eqs. (36) and (37).

with the opposite momentum, respectively. In equilibrium this change is compensated by the contributions of other electrons. But the increase of the mean-squared component of electron momentum along field gives the finite positive contribution to the total current. The acceleration of an electron by the field in y direction increases y component of the momentum and produces the opposite direction of j_x.

The values of coefficients α_{yxy} are essentially larger than α_{xxx} and α_{xyy}. It is a consequence of the fact that the motion along y direction is collisionless unless the impurity scattering is taken into account. Obviously, the difference is more pronounced at low ζ.

It is useful to calculate the possible maximal PGE coefficient. From said above it follows that this maximum is achieved for the component $\mathrm{Re}(\alpha_{yxy})$ at low frequencies $\omega \ll 1/\tau_i$ and for clean material $\tau_i \gg \tau$. In the case of linear polarized light we have

$$j_y = -\frac{1}{48\pi} n_e e v_F \left(\frac{eEl_i}{\epsilon_F} \right)^2 \sin 2\theta, \tag{40}$$

where n_e is the electron concentration, $l_i = v_F \tau_i$, θ is the angle of electric field with respect to the x direction. The estimation gives the value $j_y \sim 10^{-5}$ A/cm for $l_i = 10^{-3}$ cm, $n_i = 10^{12}$ cm^{-2}, $v_F \sim 10^7$ cm/s.

We have restricted ourselves by the classical consideration only. Two quantum factors have not been taken into account: comparability of $\hbar\omega$ with characteristic electron energies, the Fermi energy and the temperature, and the quantum corrections to conductivity. It should be emphasized that in used approximation the PGE in the metal case does not depend on the temperature in the low temperature limit because the momentum relaxation in metal is temperature independent (unlike energy relaxation). Despite the involvement of energy relaxation into the control on the distribution function, the current in the second order in electric field is determined by the contributions which do not depend on energy relaxation. This is not the case in the limit of zero impurity concentration or/and zero frequency: the nonanalytic behavior of photogalvanic tensor can be limited by inelastic scattering taking into account.

The quantum corrections suppress the low temperature transport and should lead to the temperature dependence of

the effect. Both modeling of Refs. 26 and 27 and the present theory neglect quantum corrections. Thereupon, the temperature dependence of steady current in Refs. 26 and 27 is not clear. The approach of these papers used a friction force essentially depending on the excess electron energy. Possibly, it is the reason of the temperature dependence. It should be mentioned that the quantum corrections are of less importance in high-mobility samples utilized usually in experiments with antidots.

V. COMPARISON WITH NUMERICAL SIMULATIONS

In this section we compare our results with the simulations of the flow velocity of a particle colliding with semidisks.[28] We consider the model used here as a simplification of the semidisks model of Ref. 28. The essential differences between approaches of Ref. 28 and the present paper are: periodic or random distribution of asymmetric scatterers, deterministic or chaotic character of electron scattering on antidots and motion between them, and absence or presence of the gas approximation. However, the case of low density of semidisks and weak friction corresponds to the gas approximation because the scattering randomizes the motion well enough, and the results of both approaches should be in accordance with each other.

Another important difference between two models is the finite cross section of semidisk compared with zero y cross section of the cut that provides strong angular dependence of relaxation rate $\propto \cos\phi$. However, the ordered distribution of semidisks like rectangular or hexagonal lattice possesses the "corridors" along which the relaxation vanishes as cosine of the angle towards the corridor axis. This is just the same dependence as in the case of cuts. Hence, our model can be treated as a simulation of semidisk model.

Figure 6 in Ref. 28 shows approximate quadratic dependence of the flow velocity on the alternating field what agrees with the second order in field approximation used in the present paper.

The dependence Fig. 7 from Ref. 28 demonstrates the drop of the flow velocity with the growth of the semidisk size. This behavior qualitatively corresponds to the drop $\alpha_{xxx} \to 0$ for $\tau \to 0$ (Fig. 2 of the present paper). At the same time there is no drop in this figure for large $\tau \to \infty$ following from the present paper.

The dependence of the flow velocity on the distance between semidisk centers (Fig. 8 from Ref. 28) can be treated as rescaled dependence of α_{xxx} on the mean free time τ which in the present case vanishes both for $\tau \to 0$ and $\tau \to \infty$ (Fig. 2 of the present paper).

The dependence of the flow velocity (Fig. 9 in Ref. 28) on the impurity scattering also has a drop for $\tau_i \to 0$, like expected from the Eq. (24), but there is no drop in this figure for large τ_i.

Hence, there is a partial qualitative accordance between the present results and computer simulations of Ref. 28. The origin of discrepancy needs additional study.

VI. CONCLUSIONS

The considered system of oriented asymmetric scatterers-cuts has α_{xxx}, α_{xyy}, and α_{yxy} nonzero components of photogalvanic tensor. The linear photogalvanic effect is determined by α_{xxx}, α_{xyy}, and $\mathrm{Re}(\alpha_{yxy})$. The circular-polarized illumination causes only the response of the y component of current determined by $\mathrm{Im}(\alpha_{yxy})$. The static limit of the current in impurity-free system is ambiguous, depending on value of the product of frequency to the impurity mean-free time. The x component of the current is limited and in the impurity-free system tends to zero, while the y component tends to infinity. This is explained by the accumulation of electrons in the state with zero x component of momentum.

ACKNOWLEDGMENTS

The authors are grateful to D. L. Shepelyansky and A. D. Chepelyansky for numerous helpful discussions of the problem. The work was supported by grants of RFBR Nos. 05-02-16939 and 04-02-16398, Program for support of scientific schools of the Russian Federation No. 593.2003.2 and INTAS No. 03-51-6453.

[1] D. Weiss, M. L. Roukes, A. Menschig, P. Grambow, K. von Klitzing, and G. Weimann, Phys. Rev. Lett. **66**, 2790 (1991).
[2] G. M. Gusev, Z. D. Kvon, V. M. Kudryashov, L. V. Litvin, Y. V. Nastaushev, V. T. Dolgopolov, and A. A. Shashkin, JETP Lett. **54**, 364 (1991) [Pis'ma Zh. Eksp. Teor. Fiz. **54**, 369 (1991)].
[3] Z. D. Kvon, O. Estibals, A. Y. Plotnikov, J. C. Portal, and A. I. Toropov, Physica E (Amsterdam) **13**, 752 (2002).
[4] J. Eroms, M. Tolkiehn, D. Weiss, U. Rössler, J. De Boeck, and G. Borghs, Europhys. Lett. **58**, 569 (2002).
[5] F. Galton, *Natural Inherritance* (Macmillan, London, 1889).
[6] I. P. Kornfeld, S. V. Fomin, and Ya. G. Sinai, *Ergodic Theory* (Springer, Berlin, 1982).
[7] R. Fleischmann, T. Geisel, and R. Ketzmerick, Phys. Rev. Lett. **68**, 1367 (1992); Europhys. Lett. **25**, 219 (1994).
[8] A. A. Bykov, G. M. Gusev, Z. D. Kvon, V. M. Kudryashev, and V. G. Plyukhin, Pis'ma Zh. Eksp. Teor. Fiz. **53**, 407 (1991) [JETP Lett. **53**, 427 (1991)].
[9] E. M. Baskin, M. D. Blokh, M. V. Entin, and L. I. Magarill, Phys. Status Solidi B **83**, K97 (1977).
[10] E. M. Baskin, L. I. Magarill, and M. V. Entin, Sov. Phys. Solid State **20**, 1403 (1978).
[11] V. I. Belinicher, V. K. Malinovskii, and B. I. Sturman, Sov. Phys. JETP **46**, 362 (1977).
[12] V. I. Belinicher and B. I. Sturman, Sov. Phys. Usp. **23**, 199 (1980) [Usp. Fiz. Nauk **130**, 415 (1980)].
[13] E. L. Ivchenko and G. E. Pikus, in *Semiconductor Physics*, edited by V. M. Tushkevich and V. Ya. Frenkel (Cons. Bureau, New York, 1986), p. 427.
[14] E. L. Ivchenko and G. E. Pikus, *Superlattices and Other Heterostructures*, Springer Series in Solid-State Sciences, Vol. 110 (Springer, Berlin, 1997).
[15] E. M. Baskin and M. V. Entin, JETP Lett. **48**, 601 (1988).

[16] R. P. Feynman, R. B. Leighton, and M. Sands, *The Feynman Lectures on Physics* (Addison-Wesley, Reading, MA, 1966), Vol. 1, Chap. 46.
[17] R. D. Astumian and P. Hänggi, Phys. Today **55**(11), 33 (2002).
[18] P. Reimann, Phys. Rep. **361**, 57 (2002).
[19] J. B. Majer, J. Peguiron, M. Grifoni, M. Tusveld, and J. E. Mooij, Phys. Rev. Lett. **90**, 056802 (2003).
[20] J. E. Villegas, S. Savel'ev, F. Nori, E. M. Gonzalez, J. V. Anguita, R. Garcia, and J. L. Vicent, Science **302**, 1188 (2003).
[21] A. V. Ustinov, C. Coqui, A. Kemp, Y. Zolotaryuk, and M. Salerno, Phys. Rev. Lett. **93**, 087001 (2004).
[22] C. Mennerat-Robilliard, D. Lucas, S. Guibal, J. Tabosa, C. Jurczak, J.-Y. Courtois, and G. Grynberg, Phys. Rev. Lett. **82**, 851 (1999).
[23] S. Matthias and F. Müller, Nature (London) **424**, 53 (2003).
[24] V. Studer, A. Pepin, Y. Chen, and A. Ajdari, Analyst (Cambridge, U.K.) **129**, 944 (2004).
[25] F. Jülicher, A. Ajdari, and J. Prost, Rev. Mod. Phys. **69**, 1269 (1997).
[26] A. D. Chepelianskii and D. L. Shepelyansky, Phys. Rev. B **71**, 052508 (2005).
[27] G. Cristadoro and D. L. Shepelyansky, Phys. Rev. E **71**, 036111 (2005).
[28] A. D. Chepelianskii, cond-mat/0509679 (unpublished).
[29] C. Joachim and M. A. Ratner, Proc. Natl. Acad. Sci. U.S.A. **102**(25), 8801 (2005).
[30] A. Lorke, S. Wimmer, B. Jager, and J. P. Kotthaus, EP2DS-12, Tokyo, 1997, Conference Workbook, p. 105; Physica B **249-251**, 312 (1998). For other examples of ballistic rectifiers, see also A. M. Song, A. Lorke, A. Kriele, J. P. Kotthaus, W. Wegscheider, and M. Bichler, Phys. Rev. Lett. **80**, 3831 (1998); S. de Haan, A. Lorke, J. P. Kotthaus, M. Bichler, and W. Wegscheider, Physica E (Amsterdam) **21**, 916 (2004); T. Muller, A. Wurtz, and A. Lorke, Appl. Phys. Lett. **87**, 042104 (2005).
[31] L. I. Magarill, Physica E (Amsterdam) **9**, 652 (2001).
[32] Z. D. Kvon, J. Zhang, S. Vitkalov, A. E. Plotnikov, J. C. Portal, and A. Wieck (private communication).